Dissipative collisions in ^{16}O + ^{27}Al at E_{lab} = 116 MeV

C. Bhattacharya,[1] K. Mullick,[1] S. Bhattacharya,[1] K. Krishan,[1] T. Bhattacharjee,[1] P. Das,[1] S. R. Banerjee,[1] D. N. Basu,[1] A. Ray,[1] S. K. Basu,[1] and M. B. Chatterjee[2]

[1]*Variable Energy Cyclotron Centre, 1/AF Bidhan Nagar, Kolkata 700 064, India*

[2]*Saha Institute of Nuclear Physics, 1/AF Bidhan Nagar, Kolkata 700 064, India*

(Received 15 July 2002; published 1 October 2002)

The inclusive energy distributions of fragments ($3 \leqslant Z \leqslant 7$) emitted in the reaction ^{16}O+ ^{27}Al at E_{lab} = 116 MeV have been measured in the angular range $\theta_{lab} = 15° - 115°$. A nonlinear optimization procedure using multiple Gaussian distribution functions has been proposed to extract the fusion-fission and deep-inelastic components of the fragment emission from the experimental data. The angular distributions of the fragments, thus obtained, from the deep-inelastic component are found to fall off faster than those from the fusion-fission component, indicating shorter lifetimes of the emitting dinuclear systems. The lifetimes of the intermediate dinuclear configurations have been estimated using a diffractive Regge-pole model. The lifetimes thus extracted [$\sim(1-5)\times10^{-22}$ sec] are found to decrease with the increase in the fragment charge. Optimum Q values are also found to increase with increasing charge transfer, i.e., with the decrease in fragment charge.

DOI: 10.1103/PhysRevC.66.047601 PACS number(s): 25.70.Jj, 24.60.Dr, 25.70.Gh

The phenomenon of fragment emission in light heavy-ion collisions at energies $\leqslant 10$ MeV/nucleon has evolved a lot of interest in the recent years (see Ref. [1], and references therein). The origin of these fragments extends from quasi-elastic (QE)/projectile breakup [2,3], deep-inelastic (DI) transfer and orbiting [4–10], to fusion-fission (FF) [1,10–15] processes; and in some cases the structure of the nuclei has been found to play an important role. The distinction between different reaction mechanisms, in general, and the DI and FF processes, in particular, is very difficult for light system ($A_{cn} \leqslant 40$) [1,10] as in these cases there is a strong overlap in the elemental distributions of the fragment emitted in the two processes. The DI components are characterized by large energy damping, and the fully damped yields, in general, correspond to the FF components. The energy damping observed in the DI processes is due to the manifestation of nuclear viscosity. Thus, by a systematic study of the DI fragments, it is possible to extract information on the nuclear viscosity parameters that are important for understanding nuclear fission dynamics. This is usually accomplished by studying the systematics of optimum Q values vs mass transfer and angle of rotation of the dinuclear complex. Thus, it is very much essential to decipher the data to extract the contribution of each component (e.g., DI and FF) present in the fragment emission spectra, in order to understand the underlying reaction dynamics.

Several studies made earlier for ^{16}O + ^{27}Al system at incident energies in the range of ~60–100 MeV have indicated that fragments emitted in the reaction are mainly originating from cluster transfer [16], projectile sequential breakup [2], and multinucleon transfer [7–9] processes. The roles of direct two-body and three-body projectile breakups in the fragment emission from ^{16}O + ^{27}Al reaction in the energy range of ~70–125 MeV have also been investigated recently [3]. However, none of the earlier workers did attempt to estimate the contribution of fusion-fission process as a competing process for fragment emission in ^{16}O + ^{27}Al reaction. It is well established, both theoretically [10,17] and experimentally (e.g., Ref. [1]), that for systems lying below the Businaro-Gallone point, asymmetric fission of the compound nucleus contributes significantly in the fragment emission scenario. In the present work, we have studied the fragment emission spectra from the reaction ^{16}O + ^{27}Al at E_{lab} = 116 MeV, and we report here on a simple prescription to extract the FF and the DI components of the fragment yield following the decay of light composite systems ($A_{cn} \leqslant 43$).

The experiment was performed using a 116-MeV ^{16}O^{5+} ion beam from the Variable Energy Cyclotron at Kolkata, which was recently upgraded with electron cyclotron resonance heavy-ion source. The target used was 420 μg/cm^2 self-supporting ^{27}Al. The fragments were detected using three solid state [Si(surface barrier)] telescopes (~12-μm ΔE, 300-μm E) mounted in one arm of the 91.5-cm scattering chamber. Typical solid angle subtended by each detector was ~0.3 msr. A monitor detector [~300-μm Si(surface barrier)] was placed in the other arm of the scattering chamber for normalization purpose. The telescopes were calibrated using an elastically scattered ^{16}O ion from Au target and an α particle from (Th-α) source. Typical energy resolution obtained for the elastic ^{16}O peak was ~375 keV.

Inclusive energy distributions for various fragments ($3 \leqslant Z \leqslant 7$) were measured in the angular range 15°–115°. The energy spectra of the emitted fragments ($3 \leqslant Z \leqslant 7$) have been shown in Fig. 1 for $\theta_{lab} = 20°$. The systematic errors in the data, arising from the uncertainties in the measurements of the solid angle, target thickness, and the calibration of current digitizer have been estimated to be ≈10%.

It is evident from Fig. 1 that the shapes of the energy spectra of the heavier fragments (viz., C, N) are quite different from those of the lighter fragments, viz., Li and Be. It is mainly due to variation of the relative contributions of DI and FF processes for different fragments. We adopt the following prescription for the estimation of FF and DI components present in the spectra. The energy spectra of different fragments at each angle have been fitted with two Gaussian functions in the following way. In the first step, the FF contributions have been obtained by fitting the energy distribu-

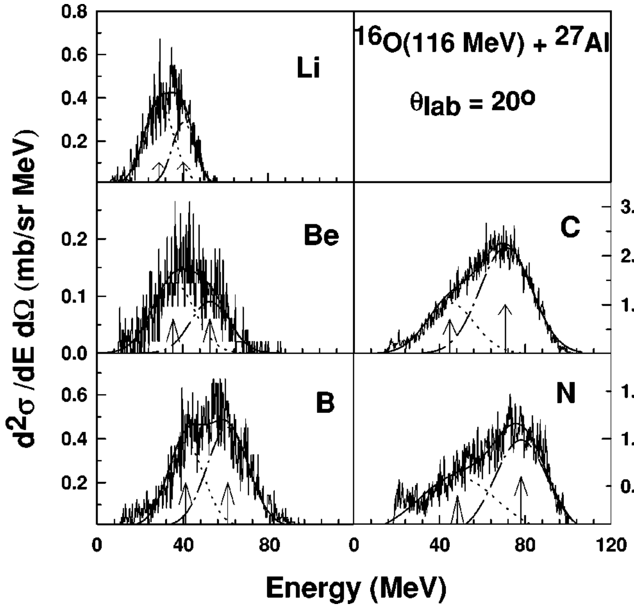

FIG. 1. Energy spectra of different fragments obtained at 20° for the $^{16}O+{}^{27}Al$ reaction (solid lines). Dotted and dash-dotted lines are the Gaussian fits to FF and DI components, respectively. Left and right arrows correspond to the centroids of the FF and DI components, respectively.

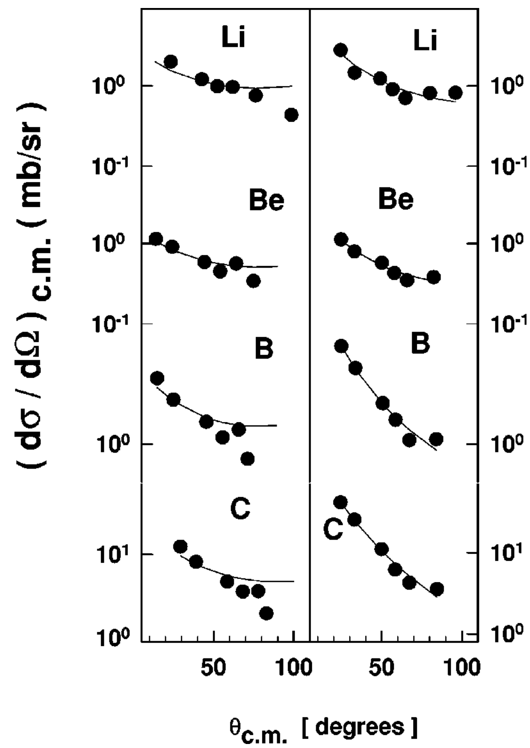

FIG. 2. Center-of-mass angular distributions of different fragments: FF component (left) and DI component (right).

tions with a Gaussian having centroid at the energies obtained from Viola systematics [18,19] of total kinetic energies of mass-symmetric fission fragments duly corrected for asymmetric factor [20]. The width of the Gaussian was obtained by fitting the lower energy tail of the spectra, assuming it to be originating purely from the FF process. The FF component of the energy spectrum thus obtained is then subtracted from the full energy spectrum. In the next step, the DI component is obtained by fitting the subtracted energy spectra with a second Gaussian. The above procedure is illustrated in Fig. 1 for the fragments ranging from Li to N at 20°. The dotted line in Fig. 1 shows the contribution of the FF component and the dashed dotted line shows the contribution of the DI component. The solid line shows the sum total contribution of both FF and DI components. In each spectrum, the arrow at lower energy corresponds to the centroid of the Gaussian for the FF component obtained from Viola systematics and the arrow at higher energy corresponds to the centroid of the Gaussian for the DI component.

The FF and the DI components of the fragment angular distributions have been obtained by integrating the respective energy distributions obtained in the manner discussed above. The center-of-mass (c.m.) angular distributions of the FF components of the fragments ($3\leqslant Z\leqslant 6$) have been displayed as a function of c.m. angle $\theta_{c.m.}$ in Fig. 2 (left). The transformation from the laboratory system to the c.m. system has been done with the assumption of a two-body kinematics averaged over the whole range of c.m. angles. The FF component has been extracted using the fission systematics [18–20] that inherently assumes that the fragments are emitted through the decay of a fully equilibrated system. Therefore, it is expected that the fragment angular distributions would reflect the same [$1/\sin\theta_{c.m.}$ type of dependence—solid lines in Fig. 2 (left)]. The total elemental yield of the FF component of the fragment emission cross sections has been compared with the theoretical estimates of the same obtained from the extended Hauser-Feshbach method (EHF) [12,20]. The EHF calculations have been performed by using a critical angular momentum value of $l_{crit}=34\hbar$ and a neck parameter consistent with the systematics given in Ref. [20]. The calculated fragment emission cross sections are shown in Fig. 3(a) as a solid histogram, and are compared with the experimental estimates of the same (filled triangles). It is seen from the figure that the theoretical predictions are in fair agreement with the experimental results.

The c.m. angular distributions of the DI components of the fragments ($3\leqslant Z\leqslant 6$) have been displayed as a function of c.m. angle $\theta_{c.m.}$ in Fig. 2 (right). A rapid fall of the angular distribution, than predicted by $1/\sin\theta_{c.m.}$ distribution, indicates a shorter lifetime of the composite system. Such lifetimes are incompatible with the formation of an equilibrated compound nucleus, but may still reflect significant energy damping within a deep-inelastic mechanism. From the measured forward peaked angular distribution, it is possible to estimate the lifetime of the intermediate dinuclear complex using a diffractive Regge-pole model [8,20]. The angular distributions are fitted with the following expression:

$$d\sigma/d\Omega=(C/\sin\theta_{c.m.})(e^{-\theta_{c.m.}/\omega t}), \tag{1}$$

and the fit to the DI component of the spectra is shown in Fig. 2 (right). This expression describes the decay of a dinucleus rotating with an angular velocity $\omega=\hbar l/\mu R^2$, where μ represents the reduced mass of the system, l its angular

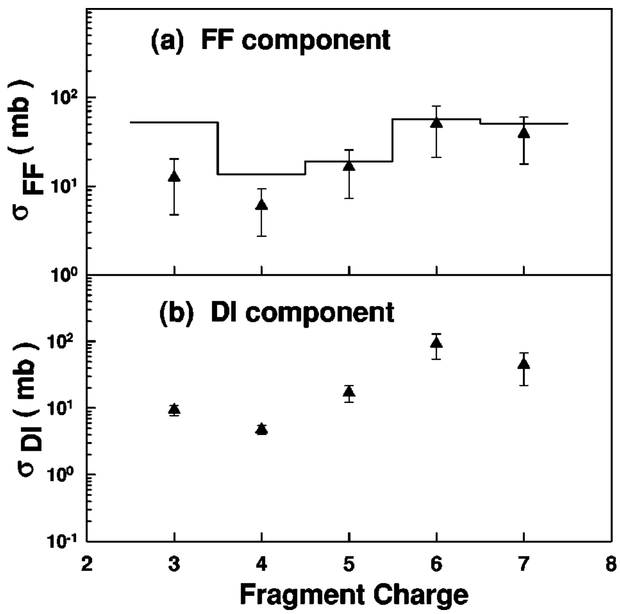

FIG. 3. Fusion-fission fragment emission cross sections. Filled triangles and solid lines correspond to the experimental and the calculated results (EHF), respectively.

momentum [which should fall somewhere between grazing (l_g) and critical (l_{cr}) angular momentum], R represents the distance between the two centers of the dinucleus, and t is the time interval during which the two nuclei remain in a solid contact in the form of the rotating dinucleus. Small values of the "life angle" $\alpha(=\omega t)$ lead to forward peaked angular distributions, associated with fast processes; whereas large values of α, associated with longer times as compared to the dinucleus rotation period $t(=2\pi/\omega)$, are consequently associated with the long-lived configurations and lead to more isotropic angular distributions. In the limiting case of very long-lived configurations, the distributions approach a $d\sigma/d\Omega \propto (1/\sin\theta_{\text{c.m.}})$ dependence. The time scales thus obtained are given in Table I for a different fragment charge Z. As found in a previous study by Mikumo *et al.* [8] for the same reaction at 88 MeV, the time scales decrease as the fragment charges increase. This is expected because the heavier fragments (nearer to the projectile) require less number of nucleon transfer and therefore less time; on the other hand, the emission of lighter fragments requires exchange of more number of nucleons, and therefore longer times. The present analysis is consistent with a recent qualitative study of the formation time in light heavy-ion reactions [21].

TABLE I. Lifetimes of the dinuclear systems for different emitted fragments.

Fragment	Li	Be	B	C	N
Time (10^{-22} sec)	4.7	3.5	1.9	1.1	0.8

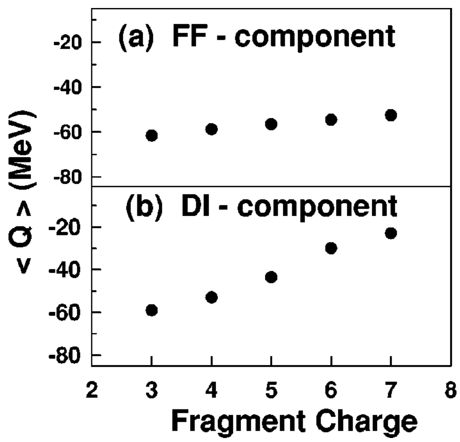

FIG. 4. $\langle Q \rangle$ value for FF and DI components of different fragments.

In Fig. 4, the optimum Q values ($\langle Q \rangle$) generated for the FF and DI components of different fragments have been plotted as a function of the fragment charge Z for a typical angle $\theta_{lab}=20°$. From the figure, it is observed that $\langle Q \rangle$ for the FF fragments is more negative than for the DI components, and does not show much variation. This is due to the fact that for the FF process, energy relaxation is complete and the system is fully equilibrated. The small variation in $\langle Q \rangle$ is due to the variation of mass asymmetry of the fragments. In case of the DI component, the large variation in $\langle Q \rangle$ values is due to the different extent of energy damping corresponding to a variation in the degree of mass transfer. Similar results have been observed at lower incident energies for the same reaction [4,8,9,16]. However, the ($\langle Q \rangle$) for each fragment is much higher than those observed earlier [8,9,16] at lower projectile energies. Such energy dependence of ($\langle Q \rangle$) may be due to the long lifetime of the dinuclear system.

The total fusion-fission (σ_{FF}) and the total deep-inelastic (σ_{DI}) cross sections for different fragments have been obtained by integrating the energy distribution of the fusion-fission component and the DI component, respectively (as discussed earlier), over the corresponding energies and over the measured angles. The cross sections thus obtained for different fragments have been displayed in Figs. 3(a) and 3(b), respectively, as a function of fragments Z. Total uncertainties in the estimation of σ_{FF} due to the experimental threshold and the limited angular range of the data have been shown by the error bars in Fig. 3. It has been found that a large fraction of C and N cross section is due to the DI mechanism.

In conclusion we have measured the inclusive double-differential cross sections for fragments emitted in the reactions $^{16}O+^{27}Al$ at $E_{lab}=116$ MeV. Total emission cross sections for various fragments have been deduced from the double-differential cross-section data. The shapes of the energy spectra of lighter fragments, e.g., Li and Be, are quite different from those of the heavier fragments. This may be due to additional contributions of QE and DI components in the spectra of heavier fragments. Besides, Li and Be experimental spectra may also have contributions from secondary deexcitation of the heavier primary excited fragments. The angular distributions of the FF component for different fragments are in fair agreement with a $(1/\sin\theta_{\rm c.m.})$ type of dependence, as they were assumed to have originated from fissionlike decay of equilibrated compound nucleus. The predicted fragment emission cross sections using the extended Hauser-Feshbach method are in fair agreement with the FF component of the same extracted from the data. The angular distributions of the DI components (laboratory grazing angle $\theta_{gr}\sim 10°$) have been fitted using the function $(C/\sin\theta_{\rm c.m.})\times(e^{-\theta_{\rm c.m.}/\omega t})$ and the time scales for the emission of different fragments have been estimated. The emission time is found to decrease as the fragment charge increases, which is expected to be justified intuitively. The total fusion-fission and deep-inelastic cross sections for different fragments have been obtained by integrating the energy distribution of the fusion-fission component and the DI component (as discussed in the text) over the corresponding energies and over the measured angles. Although a large fraction of C and N cross section is due to the DI mechanism, the FF process is found to be rather competitive in the $^{16}O+{}^{27}Al$ reaction, in agreement with the previous studies of the neighboring $^{16}O+{}^{28}Si$ system [10].

The authors thank the accelerator operation staff of the VECC for the smooth running of the machine, and staff of the target and detector laboratories for providing the targets and the Si detectors. They are thankful to C. Beck for his constructive comments. One of the authors (K.M.) acknowledges with thanks the financial support received from C.S.I.R., India.

[1] S.J. Sanders, A. Szanto de Toledo, and C. Beck, Phys. Rep. **311**, 487 (1999).
[2] N. Carlin-Filho *et al.*, Phys. Rev. C **40**, 91 (1989).
[3] S.J. Padalino *et al.*, Phys. Rev. C **41**, 594 (1990).
[4] D. Shapira *et al.*, Phys. Rev. C **21**, 1824 (1980).
[5] B. Shivakumar, S. Ayik, B.A. Harmon, and D. Shapira, Phys. Rev. C **35**, 1730 (1987).
[6] D. Shapira, R. Novotny, Y.C. Chan, K.A. Erb, J.L.C. Ford, Jr., J.C. Peng, and J.D. Moses, Phys. Lett. **114B**, 111 (1982).
[7] T.M. Cormier, A.J. Lazzarini, M.A. Neuhausen, A. Sperduto, K. Van Bibber, F. Videbaek, G. Young, E.B. Bium, L. Herreid, and W. Thoms, Phys. Rev. C **13**, 682 (1976).
[8] T. Mikumo *et al.*, Phys. Rev. C **21**, 620 (1980).
[9] M. Sato *et al.*, Phys. Rev. C **27**, 2621 (1983).
[10] A. Szanto de Toledo, S.J. Sanders, and C. Beck, Phys. Rev. C **56**, 558 (1997).
[11] S.J. Sanders, Phys. Rev. C **44**, 2676 (1991).
[12] T. Matsuse, C. Beck, R. Nouicer, and D. Mahboub, Phys. Rev. C **55**, 1380 (1997).
[13] A.K. Dhara, C. Bhattacharya, S. Bhattacharya, and K. Krishan, Phys. Rev. C **48**, 1910 (1993).
[14] C. Bhattacharya, D. Bandyopadhyay, G.S.N. Murthy, Y.P. Viyogi, S.K. Basu, K. Krishan, S. Bhattacharya, S. Kailas, A. Chatterjee, and P. Singh, Phys. Rev. C **52**, 798 (1995).
[15] C. Bhattacharya, D. Bandyopadhyay, S.K. Basu, S. Bhattacharya, K. Krishan, A. Chatterjee, S. Kailas, and P. Singh, Phys. Rev. C **54**, 3099 (1996).
[16] J.W. Harris *et al.*, Phys. Rev. Lett. **38**, 1460 (1977).
[17] L.G. Moretto, Nucl. Phys. **A247**, 211 (1975).
[18] V.E. Viola, K. Kwiatkowski, and M. Walker, Phys. Rev. C **31**, 1550 (1985).
[19] C. Beck *et al.*, Phys. Rev. C **54**, 227 (1996).
[20] C. Beck *et al.*, Eur. Phys. J. A **2**, 281 (1998).
[21] A. Szanto de Toledo, B.V. Carlson, C. Beck, and M. Thoennessen, Phys. Rev. C **54**, 3290 (1996).